

## Rapid biaxial texture development during nucleation of MgO thin films during ion beam-assisted deposition

Rhett T. Brewer<sup>a)</sup> and Harry A. Atwater

Thomas J. Watson Laboratory of Applied Physics, California Institute of Technology, Pasadena, California 91125

(Received 8 February 2002; accepted for publication 5 March 2002)

We propose a mechanism for the nucleation of highly aligned biaxially textured MgO on amorphous Si<sub>3</sub>N<sub>4</sub> during ion beam-assisted deposition. Using transmission electron microscopy, reflection high-energy electron diffraction, energy dispersive x-ray analysis, and ellipsometry, we have observed that highly aligned biaxially textured grains emerge from a “diffraction-amorphous” film when the film thickens from 3.5 to 4.5 nm. Transmission electron microscopy dark-field images also show the onset of rapid grain growth during this same film thickness interval. These results suggest biaxial texturing through aligned solid phase crystallization. © 2002 American Institute of Physics. [DOI: 10.1063/1.1476385]

Biaxially textured MgO is technologically interesting since it provides a suitable path for silicon integration of single-crystal-like films on amorphous substrates for many important perovskite oxide thin-film materials. Single-crystalline MgO (001) has already been used as a substrate for BaTiO<sub>3</sub> and Pb(Zr,Ti)O<sub>3</sub> heteroepitaxy.<sup>1,2</sup> Ion beam-assisted deposition (IBAD) creates biaxially textured films (polycrystalline films with a preferred in-plane and out-of-plane grain orientation) on amorphous substrates.<sup>3</sup> Incorporation of biaxially textured ferroelectric films with silicon integrated circuits would enable new types of actuators for microelectrical mechanical systems. Previous work has demonstrated high-quality heteroepitaxy of perovskites on Si,<sup>4</sup> but typical integrated circuit fabrication processes do not leave single-crystal Si available for oxide heteroepitaxy. By eliminating the requirement for a pre-existing heteroepitaxial template, IBAD MgO may provide an opportunity to incorporate ferroelectric materials on top of amorphous dielectric films in silicon integrated circuits following interconnect fabrication.

In contrast to materials like yttria-stabilized zirconia (YSZ) where biaxial texture evolves slowly during one micron of IBAD growth,<sup>5</sup> the biaxial texture of IBAD MgO develops rapidly during the nucleation phase. Biaxial texturing mechanisms such as anisotropic sputtering, ion channeling, and anisotropic grain damage<sup>6,7</sup> have been proposed to explain biaxial texture evolution during growth of YSZ, but do not specifically address the nucleation-mediated biaxial texturing seen for MgO. It has been suggested that IBAD MgO grains nucleate with biaxial texture because surface energy is minimized with a (001) fiber texture, leaving in-plane alignment to be achieved by ion channeling along the [011] zone axis.<sup>3</sup> High-temperature physical vapor deposition of MgO on amorphous SiO<sub>2</sub> favors nucleation with a (001) fiber texture,<sup>8</sup> but kinetic limitations result in nucleation with random orientation at room temperature.<sup>9</sup>

We have used transmission electron microscopy (TEM), electron dispersive x-ray analysis (EDAX), ellipsometry,

and *in situ* reflection high-energy electron diffraction (RHEED) to investigate IBAD MgO biaxial texture during the first few nanometers of film growth. Using electron-beam evaporation, films of MgO were deposited by room-temperature IBAD onto 30 nm thick Si<sub>3</sub>N<sub>4</sub> TEM windows at the rate of 0.17 nm/s with simultaneous ion bombardment of 750 eV Ar<sup>+</sup> ions from a Kaufman ion gun. The ions impinged on the surface at a 45° incidence angle with an ion/MgO molecule flux ratio of 0.43. The growth of each sample was stopped when the RHEED image exhibited the desired relative contributions from diffraction rings and spots. RHEED was performed with 25 keV electrons at a 2.6° incidence angle and images were taken with a 16-bit dynamic range, 1024×1024 pixels, charge coupled device camera. In order to increase the sensitivity to weak diffraction intensities, the diffuse RHEED background was removed by subtracting a RHEED image of the amorphous Si<sub>3</sub>N<sub>4</sub> substrate from all subsequent RHEED images.

RHEED pattern development for IBAD MgO grown on amorphous Si<sub>3</sub>N<sub>4</sub> is shown in Fig. 1. Film thicknesses were determined by measuring the final MgO film thickness by ellipsometry and then assuming a constant growth rate. The evolution from diffraction rings [Fig. 1(a)] to diffraction

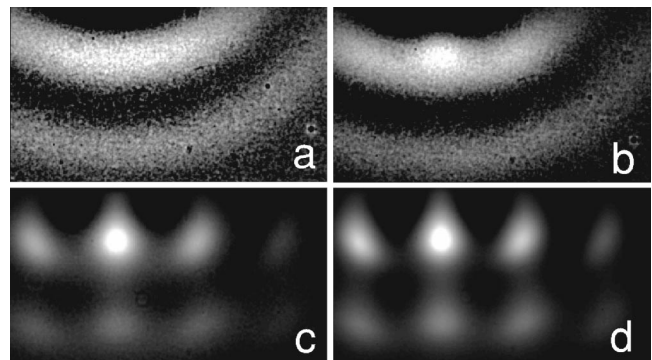


FIG. 1. *In situ* RHEED images from a continuous IBAD MgO growth experiment where the film thickness is equal to: 2.5 nm (a), 3.1 nm (b), 3.6 nm (c), and 4.2 nm (d). The field of view contains diffraction spots from (024), in the upper left-hand side corner, to (046) in the lower right-hand side corner.

<sup>a)</sup>Electronic mail: rhett@its.caltech.edu

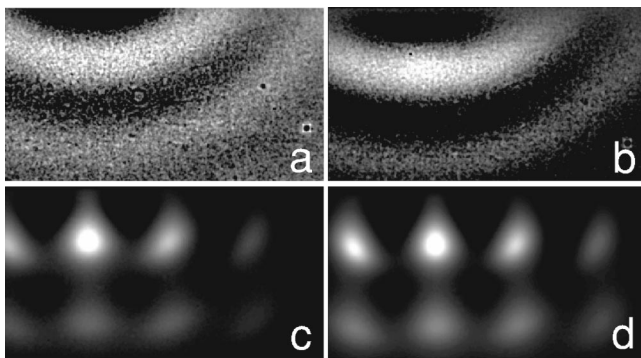


FIG. 2. RHEED images from different IBAD MgO films grown to: 1.9 nm (a), 3.7 nm (b), 4.6 nm (c), and 4.8 nm (d). The field of view contains diffraction spots from (024), in the upper left-hand side corner, to (046) in the lower right-hand side corner.

spots [Fig. 1(d)] has been observed for IBAD MgO film growths with ion energies varying from 500 to 1100 eV and ion MgO flux ratios from 0.21 to 0.57. Observations of RHEED pattern development during ion bombardment of the Si<sub>3</sub>N<sub>4</sub> substrate without MgO deposition confirm that the broad diffraction rings do not originate from the ion beam modification of the substrate.

IBAD MgO films, grown to thicknesses of 1.9, 3.7, 4.6, and 4.8 nm, were analyzed with RHEED and TEM in an effort to elucidate the development of biaxial texture during the nucleation phase. RHEED images from these samples (Fig. 2) show that the RHEED pattern development for these films follows the same evolution as observed for the single continuous growth (Fig. 1). The transition from broad diffraction rings to diffraction spots begins at 3.7 nm [Fig. 2(b)] and is finished by 4.8 nm [Fig. 2(d)]. RHEED diffraction rings typically indicate a random out-of-plane orientation distribution, but the RHEED image from 1.9 nm of IBAD MgO [Fig. 2(a)] lacks rings that would be present in a randomly oriented polycrystalline film, suggesting that the film is amorphous MgO.

The transmission electron diffraction pattern of the thinnest film (1.9 nm) confirms that it is amorphous, as illustrated in Fig. 3(a). EDAX measures the amount of MgO on the surface in Fig. 3(a) to be 34% of the amount present in Fig. 3(d), corroborating the relative film thicknesses measured by ellipsometry. Atomic force microscopy measured film roughness to be 0.24 and 0.23 nm root-mean-square for the 1.9 and 3.7 nm thick IBAD MgO films shown in Figs. 3(a) and 3(b), respectively. These observations strongly suggest that the MgO films in Figs. 3(a) and 3(b) are continuous and amorphous. Only diffraction rings from (001) fiber textured grains were observed. However, the diffraction patterns show that the in-plane orientation distribution changes from random at 3.7 nm [Fig. 3(b)] to highly aligned at 4.8 nm [Fig. 3(d)]. During the rapid development of biaxial texture, rapid crystal growth also occurs. Individual grains are not observed for the 1.9 nm thick film [Fig. 3(a)], however, starting with the onset of fiber texture development, the dark-field images show progressively larger grains as shown in Figs. 3(b)–3(d). The area fraction of diffracting MgO crystalline material observed in dark-field TEM and the in-plane orientation distribution, measured using RHEED analysis,<sup>10</sup> are plotted as a function of film thickness in Fig. 4. There is

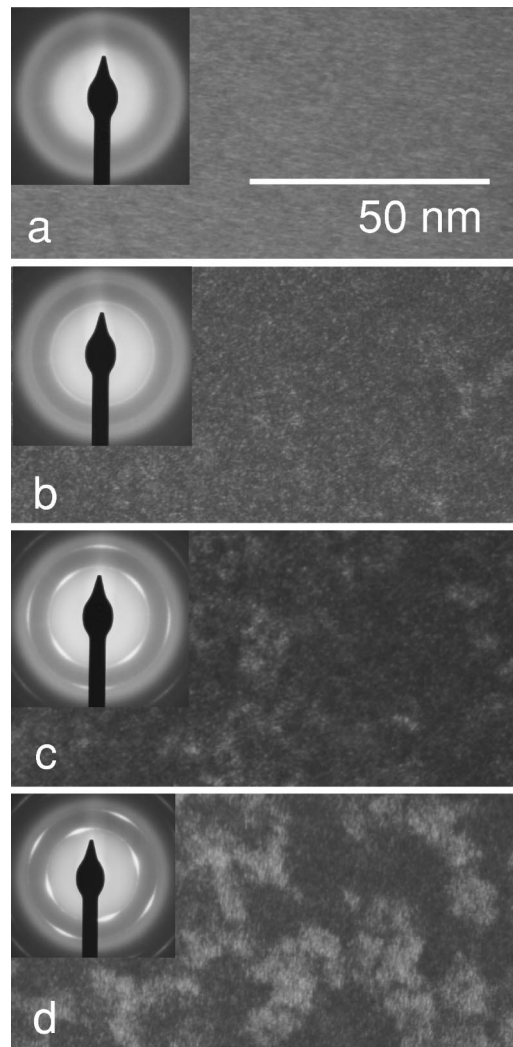


FIG. 3. TEM dark field images and diffraction patterns for IBAD MgO films with thicknesses equal to: 1.9 nm (a), 3.7 nm (b), 4.6 nm (c), and 4.8 nm (d).

a clear correlation between lateral crystal growth and biaxial texture.

The observations reported here are consistent with a three-stage microstructural evolution during IBAD: (i) an initially amorphous MgO film is deposited which remains amorphous in the thickness range between 0–3.5 nm, (ii) MgO crystals nucleate via solid phase crystallization<sup>11</sup> with

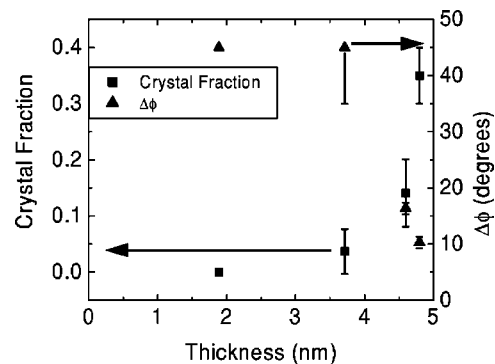


FIG. 4. Fraction of crystalline material observed for IBAD MgO with dark-field TEM as a function of film thickness. In-plane orientation distribution ( $\Delta\phi$ ) measured as a function of film thickness.

restricted out-of-plane texture and nearly random in-plane texture at a thickness of approximately 3.5 nm, and (iii) in-plane texture evolves rapidly in the thickness range between 3.5 and 4.5 nm due to amorphization of grains with misaligned in-plane texture and preferential lateral solid phase growth of grains with aligned in-plane texture. Recent molecular dynamic simulations of  $\text{Ar}^+$  ion collisions with small MgO crystals yield insights to nucleation-mediated IBAD biaxial texture development. Molecular dynamics simulations by Zepeda-Ruiz and Srolovitz calculate that for a single  $\text{Ar}^+$  ion impact along the [011] channeling direction (a minimum damage direction), a  $1.3 \times 1.3 \times 1.3$  nm MgO crystal is amorphized, but a  $2.1 \times 2.1 \times 2.1$  nm MgO crystal sustains little permanent damage.<sup>12</sup> It is energetically favorable for MgO to form small crystallites, however, the ion bombardment amorphizes and laterally distributes the material from the first crystals, even those aligned along ion channeling directions. Once the film reaches a critical thickness, there is enough material for stable-sized MgO crystals to form. We suggest that surface-free energy minimization, coupled with energy from ion collisions, drives the out-of-plane orientation toward a (001) fiber texture.<sup>13</sup> There is no energetically favorable in-plane orientation for nucleation on an amorphous substrate and so the MgO crystals nucleate in the amorphous MgO matrix with a random in-plane orientation distribution. Crystals which have the [011] zone axis aligned along the direction of the incoming  $\text{Ar}^+$  ions receive less damage than misaligned crystals, which can be locally amorphized by ion bombardment<sup>7</sup> and effectively prevented from growing. As a result, solid phase crystallization proceeds around grains which are oriented with a (001) fiber texture and an in-plane orientation that faces the [011] zone axis toward the incoming ions, creating a biaxially textured MgO thin film.

Sensitive RHEED experiments and subsequent TEM analysis revealed an abrupt, unexpected transition from an amorphous film to a biaxially textured film. These results clearly show that anisotropic ion damage, not anisotropic ion sputtering, is responsible for nucleating biaxially textured IBAD MgO films. The experimental observations are consistent with the appearance of biaxial texture from an initially amorphous layer of MgO through solid phase crystallization around biaxially textured seed grains.

This work was supported by the DARPA VIP III program, ARO MURI Grant No. DAAD 19-01-1-0517, and the Intel Foundation.

- <sup>1</sup>W. J. Lin, T. Y. Tseng, H. B. Lu, S. L. Tu, S. J. Yang, and J. N. Lin, *J. Appl. Phys.* **77**, 6466 (1995).
- <sup>2</sup>N. Wakiya, K. Kuroyanagi, Y. Xuan, K. Shinozaki, and N. Mizutani, *Thin Solid Films* **357**, 166 (1999).
- <sup>3</sup>C. P. Wang, K. B. Do, M. R. Beasley, T. H. Geballe, and R. H. Hammond, *Appl. Phys. Lett.* **71**, 2955 (1997).
- <sup>4</sup>R. A. McKee, F. J. Walker, and M. F. Chisholm, *Phys. Rev. Lett.* **81**, 3014 (1998).
- <sup>5</sup>J. Wiesmann, J. Dzick, J. Hoffmann, K. Heinemann, and H. C. Freyhardt, *J. Mater. Res.* **13**, 3149 (1998).
- <sup>6</sup>L. S. Yu, J. M. E. Harper, J. J. Cuomo, and D. A. Smith, *J. Appl. Phys.* **60**, 4160 (1986).
- <sup>7</sup>L. Dong and D. J. Srolovitz, *J. Appl. Phys.* **84**, 5261 (1998).
- <sup>8</sup>J. S. Lee, B. G. Ryu, H. J. Kwon, Y. W. Jeong, and H. H. Kim, *Thin Solid Films* **354**, 82 (1999).
- <sup>9</sup>M. O. Aboelfotoh, *Appl. Phys. Lett.* **24**, 347 (1974).
- <sup>10</sup>R. T. Brewer, J. R. Groves, P. N. Arendt, and H. A. Atwater, *J. Appl. Phys.* (unpublished).
- <sup>11</sup>K. T.-Y. Kung, R. B. Iverson, and R. Reif, *Appl. Phys. Lett.* **46**, 683 (1985).
- <sup>12</sup>L. A. Zepeda-Ruiz and D. J. Srolovitz, *J. Appl. Phys.* (unpublished).
- <sup>13</sup>J.-G. Yoon, H. K. Oh, and S. J. Lee, *Phys. Rev. B* **60**, 2839 (1999).